TECHNICAL PAPER

CrossMark

Hydrodynamic study of a double-stepped planing craft through numerical simulations

Parviz Ghadimi[1] · Saeid Panahi[1] · Sasan Tavakoli[1]

Abstract

This paper investigates the performance and hydrodynamic characteristics of a double-stepped planing hull and the effects of adding two steps to the bottom of a mono-hull. To study these effects, a non-stepped model with similar characteristics of a stepped hull is also modeled. The numerical simulations are conducted in different stages. First, a mesh study is performed and an optimum mesh size is adopted. Subsequently, the predicted resistances are compared against experimental data and good agreement is observed. Later, the targeted simulations are performed at five different Froude numbers and various characteristics are determined. The results of these studies indicate that frictional resistance of the double-stepped model is drastically smaller than that of the non-stepped model, while pressure drag of the stepped vessel is slightly larger than the non-stepped model. It is observed that adding steps to the hull does not reduce the wetted surface at lower Froude numbers, but its positive effect appears when Froude number exceeds 2.0. It is also seen that generated transom wave behind the double-stepped hull is larger than that of the non-stepped hull. In addition, the computed pressure distributions over the center line of both models indicate that the first maximum pressure of the double-stepped model is larger than that of the non-stepped hull. Ultimately, it is concluded that hydrostatic pressure has an essential role in producing the lift force of a non-stepped planing hull, but this pressure has very little contribution in generation of the lift force of the double-stepped hull.

1 Introduction

Planing hulls are well known for their high-speed capability and are widely used for different purposes varying from recreational to sports applications. These hulls are identified by their hydrodynamic force that contributes to supporting of their weight which in turn empowers the vessel to reach high Froude numbers. The demand for increasing their speed over time has been accompanied with various innovate ideas. Some researchers have proposed to add extra equipment to the vessel, and some have offered using steps at the bottom of the boat. When the latter idea is used, an air cavity is generated at the bottom of the boat which results in reduction of the wetted surface of the boat and yields more maximum pressure areas. Prior to twenty-first century, the stepped planing hulls were not used as much as they are being used today. Because of the fact that they were very vulnerable to exhibit instabilities, the demand for these hulls had been dropped. However, engineers have successfully designed a new generation of the stepped hulls that are much safer than earlier versions. Meanwhile, the idea of using two or even three steps instead of one step has heightened, as well. Modern experimental studies have also been conducted in order to make sure of their ability to reach high speeds with proper stability. One important point to be noted is the fact that by using these experimental studies, only limited information can be acquired regarding their performance, but there is surely an essential need to know about the flow pattern and some other hydrodynamic properties that cannot be measured through experimental studies. By conducting a numerical simulation, more insights can be gained regarding the hydrodynamic of the stepped planing hulls in an easier process.

✉ Parviz Ghadimi
  pghadimi@aut.ac.ir

[1] Department of Marine Technology, Amirkabir University of Technology, Hafez Ave, No 424, P.O. Box 15875-4413 Tehran, Iran

Hydrodynamic study of planing hulls in its early era was limited to a number of experimental and theoretical works like those which concentrated on the gage pressure measurements [1, 2] and the ones related to the highlighted hydrodynamics of planing plates [3, 4]. Researches were not extended beyond these topics and provided only flow patterns, resistance calculation and/or performance predictions due to the lack of both experimental facilities and comprehensive numerical methods in that period of time. Meanwhile, Savitsky [5] took advantage of all the previous experimental studies and presented an accumulated package of empirical relations and established a helpful mathematical approach for performance prediction and even hydrodynamic deign of the non-stepped hard-chine planing hulls. Similar approaches were adopted for performance prediction by other new researchers [6, 7]. However, in spite of the adequate accuracy and simplicity of the application, one major problem remained that all these empirically developed methods were restricted to a specified applicatory boundary and could not be used for planing hulls like stepped planing hulls which is studied in the current paper, or hulls with spray rails. Although some progress has been made in modeling the stepped hulls [8] or hulls equipped with spray rails [9], they are not significant and wide enough that can be expected to offer a suitable performance prediction for such hulls along with a proper insight regarding their hydrodynamic characteristics. Accordingly, numerical investigation of this issue may be considered a good alternative approach which can easily overcome the previous limitations.

Numerical prediction of hydrodynamic of planing hulls has been done by different researchers, and this effort has been accelerated in the recent years. Different types of planing hulls have been modeled, and proper accuracy of numerical simulations has been achieved. The first probe into advantages of numerical methods over empirical- and theoretical-based approaches in modeling the planing boats can be found in the work of Pemberton [10] who compared the results of RANS simulations against empirically based results and drew some meaningful conclusions showing the accuracy and potential of the numerical methods in modeling more real boats. Furthermore, Caponnetto [11] performed CFD analysis by implementing a $k–\varepsilon$ model and showed the good capability and acceptable accuracy of the numerical methods in modeling the planing hulls with emphasis on the flow around the boat. Another important numerical research on the performance of planing hulls was then conducted by Brizzolara and Serra [12], the results of which indicated good accuracy of the CFD codes in modeling the non-stepped planing hulls. Various CFD studies were also conducted by researchers during the last 15 years by focusing on validation and verification [13], performance prediction through transient modeling [14], tunnelled hulls [15], trim tab effects [16], and even flow pattern around

planing hulls [17, 18]. Recently, a very comprehensive CFD study was conducted by Seif et al. [19] who showed different capabilities of CFD approach such as pressure distribution, wetted surface, resistance and spray pattern prediction as well as shallow water effects in hydrodynamic modeling of planing hulls. A detailed review on these methods has also been presented by Yousefi et al. [20]. Through scrutiny of all these works, one may conclude that CFD codes have been main contributing factors to the recent progress made in the field of planing hulls. However, it is noteworthy that these works rarely focused on stepped hulls and bottom air cavity.

As pointed out earlier, the stepped planing hulls have drawn much attention from designers during the recent years. Several evidences regarding this issue can be observed in some modern experimental studies [21–24] which have been conducted on new hull series, as well. Meanwhile, Matveev [25–27] performed a series of numerical studies in which potential flow was solved to model hydrodynamics of stepped hulls. However, his numerical studies were helpful and the results were useful; since potential flow was solved, they had some limitations such as lacking the viscous effects and neglecting the stresses which can result in some significant errors. Garland and Maki [28] focused on a one-stepped planing plate and numerically modeled it by considering the viscosity effect. Although their study was constrained to a 2D plate, they presented some useful results which included pressure distribution, lift and drag forces, and free surface elevation. Their results were indicative of the fact that position of the step and its height is very important, but the lift force of a stepped planing plate in all cases is larger than that of a non-stepped plate. In addition, Makasyeyeve [29] conducted a theoretical analysis on the performance of planing plates and presented water elevation and pressure distribution over the entire length of the plate. Lotfi et al. [30] also investigated a one-stepped planing hull and validated their numerical simulations with experimental works. Meanwhile, in the recent experimental works of Taunton et al. [21] and Lee et al. [22], double-stepped planing hulls have been introduced. Through a close scrutiny of this issue, it can be seen that there is a considerable gap in numerical modeling of the double-stepped planing hulls and there is still a vital need to investigate the double-stepped planing crafts.

The current paper focuses on numerical simulation of a double-stepped planing hulls. The first considered hull is one which has been recently introduced by Taunton et al. [21]. The second studied hull has the same body plane as that of the double-stepped one. The only thing that distinguished these two crafts from each other is the existence of two transverse steps in the bottom of the stepped one. The intended numerical simulations are conducted using ANSYS-CFX software that applies finite volume method (FVM) and volume of fluid (VOF) scheme for solving multiphase problems. The $k–\varepsilon$ model is used to model the turbulence. Mesh

sensitivity analysis is performed, and the obtained results are validated against experimental data to confirm the accuracy of the proposed numerical model. Ultimately, comparisons are made between the results of the non-stepped hull and the stepped hull to gain more understanding and insight regarding the effects of the step on the performance of the boat and behavior of the flow around it. The studied parameters include the resistance force, the wetted surface, the free surface elevation, and the pressure distribution. Finally, the conclusions drawn from the current study are explained and prospects of ongoing plans are reported.

2 Problem statement

2.1 Definition of the problem

Geometry of the considered problem is sketched in Fig. 1 in which the double-stepped and the non-stepped hulls are displayed. The vessel is considered to move forward with speed of U, and the boat is constrained to move only along the longitudinal direction. The boat is assumed to have a fixed trim angle of τ and CG rise up of Z_{CG}. Values of these parameters used in the current simulation were taken directly from the experiment reported by Taunton et al. [21]. In addition, the speed is normalized using definition of the volume-based Froude number as in

$$\text{Fr} = \frac{U}{\sqrt{g\forall^{1/3}}} \tag{1}$$

where $\forall$ is the submerged volume of the vessel in zero-speed condition and g is the gravity acceleration. An overall wetted length of the keel is defined for the boat which stands for the distance between the intersection of the calm water and the keel to transom. In the case of non-stepped planing hull, this length is a continuous line, while in the case of a stepped planing hull, this length is different. A resistance force that consists of frictional, pressure, spray, and residual components act on the bottom of the vessel. To examine the flow around the vessel, different choices may be applied that can be theoretically based using 2D+T theory [31–33], or semi-empirically based [5, 8, 34], or numerical techniques. As pointed out earlier, in the current study, numerical methods are implemented.

2.2 Investigated hulls

The hull which is studied in the current paper has been previously investigated by Taunton et al. [21]. They introduced four different body planes and utilized step in one of them. The model without any step is called Model C, and the one with double steps is named Model C2. Body profiles of these two models are illustrated in Fig. 2. Principal characteristics

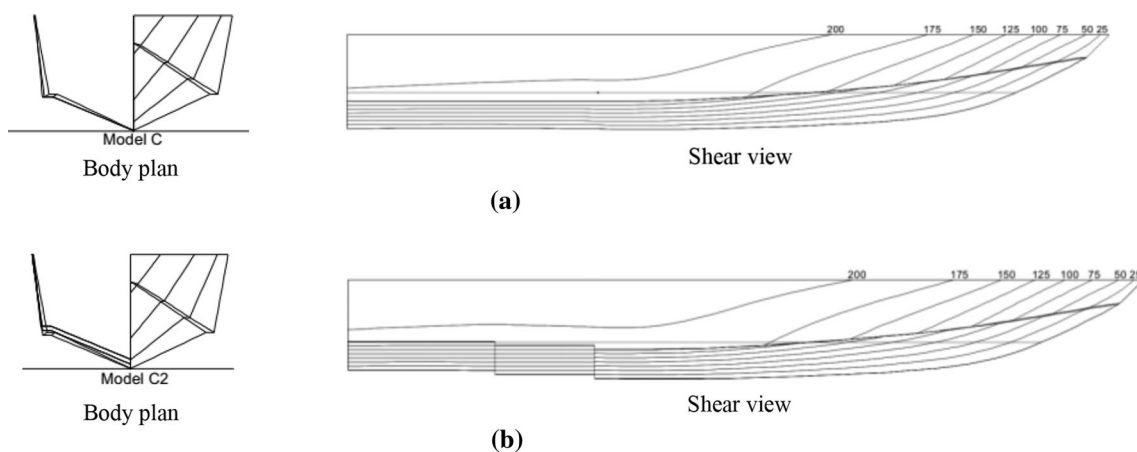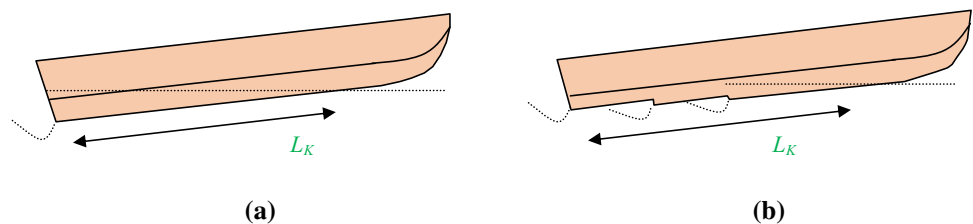**Fig. 1** **a** Non-stepped and **b** double-stepped planing hulls

Fig. 2 Body profile of **a** Model C and **b** Model C2

of these hulls are shown in Table 1. In the current paper, it is aimed to simulate flow around these hulls and subsequently compare their pressure distributions, wetted surfaces, and hull resistance.

2.3 Governing equations

In the current problem, two fluids of water and air are involved and velocity of each fluid is much smaller than speed of sound in them. Accordingly, the fluids are assumed to be incompressible and two equations of conservations of mass and momentum need to be solved. Continuity of mass is written in the form of

$$\frac{\partial \rho}{\partial t} + \frac{\partial}{\partial x_i}\left(\rho u_j\right) = 0 \tag{2}$$

where ρ is the fluid density, t represents time and u_j is the component of velocity vector along j direction. Navier–Stokes equations in its Reynolds average form is written as

$$\frac{\partial \rho u_j}{\partial t} + \frac{\partial}{\partial x_j}\left(\rho u_i u_j\right) = -\frac{\partial P}{\partial x_i} + \frac{\partial}{\partial x_j}\left(\tau_{ij} - \overline{\rho u_i' u_j'}\right) + g_i \tag{3}$$

where x_j is the coordinate in j direction, p is the gauge pressure, and g_i refers to the component of gravity vector in i direction. It should be noted that the coordinate system is defined in a way that gravity vector become zero in the directions of 1 and 2, and becomes g (9.81 m/s^2) in the direction of 3. Finally, $\rho u_i' u_j'$ is the Reynolds stress. Using the turbulent viscosity theory describing the relation between the Reynolds stress and velocity gradient, Eq. (3) can be written as follows

$$\frac{\partial \rho u_j}{\partial t} + \frac{\partial}{\partial x_j}\left(\rho u_i u_j\right) = -\frac{\partial P}{\partial x_i} + \frac{\partial}{\partial x_j}\left[\mu_{\text{eff}}\left(\frac{\partial u_i}{\partial x_j} + \frac{\partial u_j}{\partial x_i}\right)\right] + g_i \tag{4}$$

where μ_{eff} is the effective viscosity which is defined by

$$\mu_{\text{eff}} = \mu + \mu_t \tag{5}$$

Table 1 Principal characteristics of Models C and C2

	Model C	Model C2
L (m)	2.0	2.0
B (m)	0.46	0.46
Δ (N)	243.4	243.4
$L/\nabla^{1/3}$	6.86	6.86
β at transom	22.5	22.5
L_1	–	0.48
L_2	–	0.62

Since the fluids are assumed viscous and the problem deals with a high-speed craft, the Reynolds number, defined as

$$\text{Re} = \frac{UL}{\vartheta} \tag{6}$$

exceeds 10^6, and the problem is found to be turbulent. In order to model the turbulence, the k–ε model is utilized in the current study. In this model, k is the turbulent kinetic energy and ε represents the turbulent dissipation. The eddy viscosity of turbulent kinetic energy and turbulent dissipation is defined as

$$\mu_t = C_\mu \rho \frac{k^2}{\varepsilon} \tag{7}$$

where c_μ is constant, and k and ε are found by solving the continuity equation

$$\frac{\partial(\rho k)}{\partial t} + \frac{\partial}{\partial x_j}\left(\rho u_j k\right) = \frac{\partial}{\partial x_j}\left[\left(\mu + \frac{\mu_t}{\sigma_k}\right)\frac{\partial k}{\partial x_j}\right] + P_k - \rho\varepsilon \tag{8}$$

$$\frac{\partial(\rho\varepsilon)}{\partial t} + \frac{\partial}{\partial x_j}\left(\rho u_j \varepsilon\right) = \frac{\partial}{\partial x_j}\left[\left(\mu + \frac{\mu_t}{\sigma_\varepsilon}\right)\frac{\partial\varepsilon}{\partial x_j}\right] + \frac{\varepsilon}{k}(C_{\varepsilon 1}P_k - C_{\varepsilon 2}\rho\varepsilon) \tag{9}$$

In the above equation, $\sigma_k, C_{\varepsilon 2}, C_{\varepsilon 1}$ are constant and p_k is the turbulence effect caused by viscosity forces. More information regarding these equations and their derivation can be found in Ref. [34]. To analyze the defined multiphase problem, volume of fraction scheme is adopted. Through this approach, the volume fraction of air and water in each cell can be estimated. The parameters α and $(1–\alpha)$ are defined to be fractions of existence of air and water in a cell, respectively. If α is equal to 1.0, then the entire volume of the cell is assumed to be filled with air, and if α is 0.0, the cell is filled with water; otherwise, a combination of air and water exists in the volume. The equation governing the volume fraction is written as

$$\frac{\partial\alpha}{\partial t} + \vec{\nabla}\cdot(\alpha\vec{u}) = 0 \tag{10}$$

If the above equation is solved for each time step, the effective density and viscosity of a cell can be found by

$$\rho_{\text{eff}} = \alpha\rho_{\text{air}} + (1-\alpha)\rho_{\text{water}} \tag{11}$$

$$\vartheta_{\text{eff}} = \alpha\vartheta_{\text{air}} + (1-\alpha)\vartheta_{\text{water}} \tag{12}$$

3 Simulation technique

3.1 Computational approach

To investigate the problem, the ANSYS-CFX software is utilized. It applies finite element-based finite volume method for solving the momentum and mass continuity equations by

SIMPLE scheme [35]. The considered domain of the problem is illustrated in Fig. 3. It should be mentioned that the domain is considered to be rectangular which is separated into two sub-domains, consisting of the upper and lower domains. Taking advantage of the recommendations presented in Ref. [36], the distance from the planing hull from the upper and lower sides is set to be L, and the width of the region is considered to be 0.75L, while the length of the downstream region is set to be 0.5L. Also, the length of the upstream of the vessel from the outlet is considered to be 2.5L.

3.2 Generated mesh

Since the considered three-dimensional planing problem is complex and its geometry is not simple, an unstructured grid with tetrahedral cells is used in targeted numerical simulations. Two sub-domains are defined; one around the hull and the other around the free surface. Under these conditions, accuracy of the simulations is enhanced, especially in determining the free surface elevation and hydrodynamic pressure. Moreover, an edge sizing mesh is used by which the mesh cells become smaller near the free surface and the vessel. A boundary layer mesh is also implemented near the body. As a result, an inflation layer mesh with high resolution and $y+$ of about 60 is used. Five different mesh sizes are defined and an optimum mesh is found for the problem. The generated mesh is displayed in Fig. 4 where a close-up view around the steps and the transom stern are shown (Table 2).
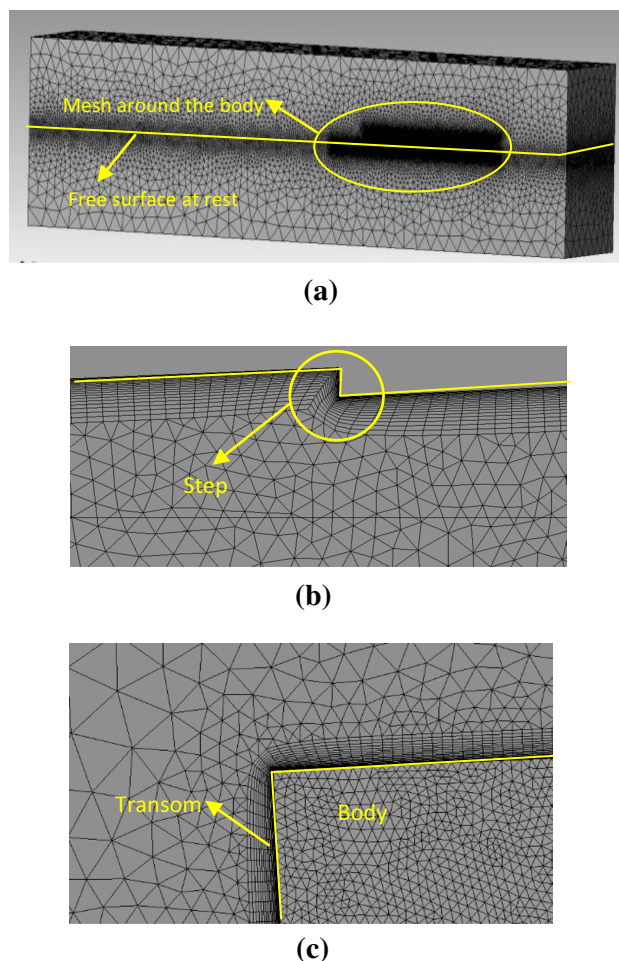
4 Results

4.1 Grid independence analysis

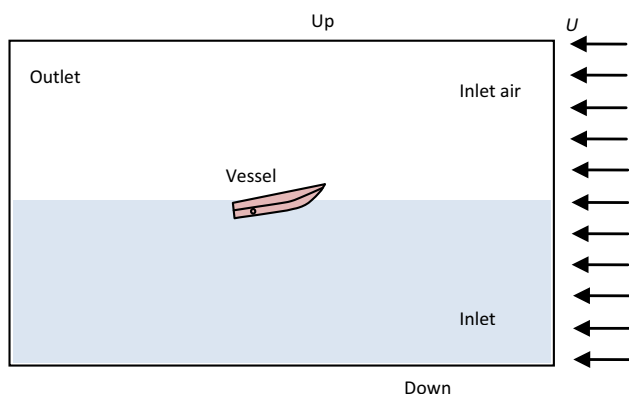Before presenting the main results, a mesh study is conducted to find an appropriate mesh size. For this purpose,

(a)

(b)

(c)

Fig. 4 The generated mesh: **a** overall view, **b** close-up view near the step, **c** close-up view near the transom

the Model C2 is numerically studied at advanced speed of 10.13 m/s which corresponds to the Froude number $Fr = 4.807$. Different numbers of cells ranging from 2.5 million to 7.4 million cells are considered, and the required simulations are performed. The computed resistance force for each of these cases is shown in Fig. 5. As seen in this figure, the drag forces are different for the first three mesh

Fig. 3 Longitudinal view of the domain (side walls are not identifiable in this figure)

Table 2 The defined boundaries and their set up

Boundary	Variable		
	U	P	α
Inlet water	$\mathbf{U} = U\mathbf{i} + 0\mathbf{j}$	$\frac{\partial}{\partial n}(P) = 0$	$\alpha = 0$
Inlet air	$\mathbf{U} = U\mathbf{i} + 0\mathbf{j}$	$\frac{\partial}{\partial n}(P) = 0$	$\alpha = 1$
Outlet	$\frac{\partial}{\partial n}(\mathbf{U}) = 0$	$P = 0$	$\frac{\partial}{\partial n}(\alpha) = 0$
Vessel	$\mathbf{U} = 0$	$\frac{\partial}{\partial n}(P) = 0$	$\frac{\partial}{\partial n}(\alpha) = 0$
Up	$\frac{\partial}{\partial n}(\mathbf{U}) = 0$	$P = 0$	$\frac{\partial}{\partial n}(\alpha) = 0$
Down & Side	$\frac{\partial}{\partial n}(\mathbf{U}) = 0$	$\frac{\partial}{\partial n}(P) = 0$	$\frac{\partial}{\partial n}(\alpha) = 0$

sizes, but the computed resistance forces for the last two cases are approximately equal. As observed in Fig. 5, the case with finest mesh (7.4 million cells) may be considered as the most adequate mesh for the current problem, since a finer mesh than this mesh size does not offer any significant variation in the drag force.

4.2 Validation

The validation of the current numerical simulation is accomplished through drag force of Model C2 at different speeds and comparing them against experimental data. The obtained results are displayed in Fig. 6. As evident in this figure, the numerical results and experimental data are in good agreement. However, large differences can only be seen at largest Froude number at where the boat reaches its high speed where the most possible turbulence occurs. Relative errors for the resistance computed at different velocities, determined by $\left|\frac{V_{exp} - V_{num}}{V_{exp}}\right| \times 100$, are presented in Table 3 to demonstrate the accuracy in each case.

Comparison of the predicted wetted surface with experimental values is also shown in Fig. 7, and the relative errors are shown in Tables 4 and 5. It can be seen that the trend of the predicted values is in good agreement with experimental data for the non-stepped hull at all speeds. However, for the double-stepped hull, the error in predicting the wetted surface increases, especially with an increase in speed. This phenomenon was also observed by the numerical simulations of DeMarco et al. [37] who numerically studied a one-stepped planing hull.

4.3 Main results

4.3.1 Resistance force

The computed resistance force for both models is shown in Fig. 8. Through close scrutiny of this figure, one may conclude that smaller force resists against model C2 at all Froude numbers. However, the difference between the
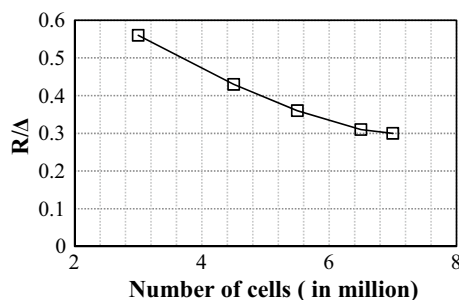
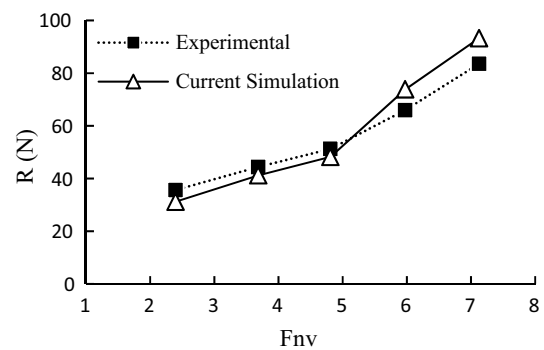**Fig. 5** Mesh study (the computed resistance force)

Fig. 6 Comparison of the predicted and experimentally measured resistance of Model C2

resistance of Models C and C2 is very little at the first two Froude numbers, while it becomes significant at two larger Froude numbers. Another important fact is the small difference of the wetted surface of these hulls at smaller Froude numbers. In cases at which Froude number is slightly larger than 1.0, step does not reduce the wetted surface as much as it does at Froude numbers much larger than 1.0. This fact is further explored in the upcoming results.

The components of the resistance consisting of the frictional and pressure drag are displayed in Fig. 9. Results in this figure imply that Model C2 has smaller frictional resistance in comparison with Model C. This is while the pressure drag of Model C is slightly smaller than that of Model C2. However, although the Frictional drag is the dominant contributor in resistance force, the resistance of Model C2 gets smaller than that of Model C.

4.3.2 The wetted surface

The computed wetted surface of both Models C and C2 is displayed in Fig. 10. It can be seen that the wetted surface of Model C2 is larger than that of C. At these speeds (Fr < 4), the flow is not separated from steps sufficient enough to yield large dry areas. However, as the speed increases, the separated flow from the step has a larger amplitude and hence reaches the bottom of the vessel after traveling larger path in comparison with lower speeds.

Table 3 Relative errors in computing the resistance force of Model C2

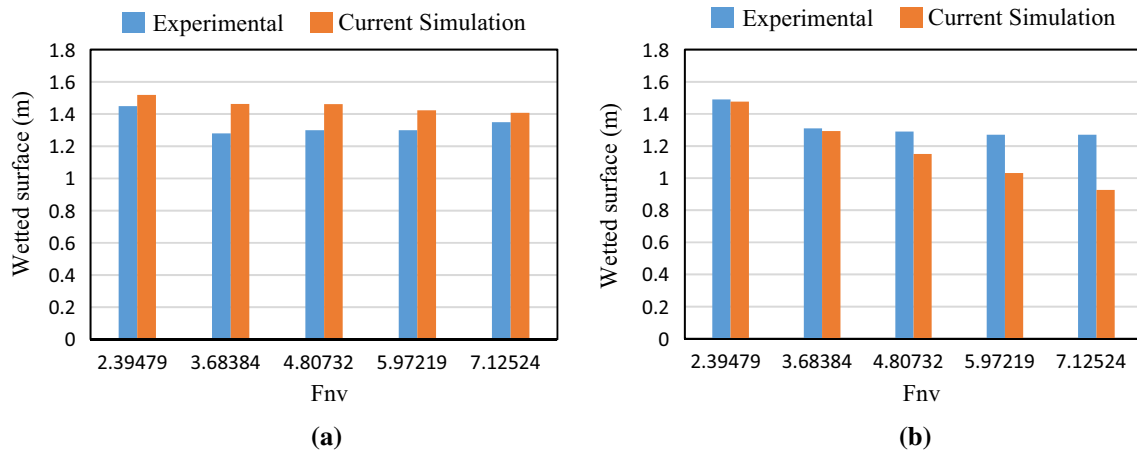| U (m/s)	Relative error
4.05	0.118993
6.25	0.059707
8.13	0.071461
10.13	0.123596
12.05	0.116218

Fig. 7 Comparison of the wetted surface between experimental data and numerical results of **a** Model C and **b** Model C2

Table 4 Relative errors in computing the wetted surface of Model C2

U (m/s)	Relative error
4.05	0.009413423
6.25	0.012860305
8.13	0.108117829
10.13	0.188137008
12.05	0.269952756

Table 5 Relative errors in computing the wetted surface of Model C

U (m/s)	Relative error
4.05	0.048075862
6.25	0.142476563
8.13	0.124715385
10.13	0.095046154
12.05	0.043288889

Fig. 8 Comparison of the resistance of Model C against Model C2

In order to provide a better understanding regarding the behavior of the wetted surface, the bottom views of the wetted surface of both considered hulls are displayed in Fig. 11. In this figure, some important points can be observed. At the lowest Froude number (Fr = 2.395), step does not significantly affect the flow separations near the chines. At Froude number Fr = 3.684, the step results in some flow separations leading to the generation of some distinct wetted area. In addition, since these areas are generated far from the center line, they certainly have smaller pressure which cannot be counted on providing enough lift. Therefore, large wetted surface is observed in the fore body. A different behavior can be seen at the other three Froude numbers of 4.807, 5.972 and 7.125. The middle body is drenched very little; however, the aft body is wetted, considerably. Where the keel of the aft body is wetted, the Froude number is relatively large, and as a result high pressure occurs at the aft body, and the wetted surface of the fore body is reduced.

4.3.3 Free surface elevation

The transverse sections of both models in the form of free surface elevation are illustrated in Fig. 12. Parameter X in each section refers to its longitudinal distance from the transom. Three sections are shown for each Froude number. These sections correspond to the aft body, the mid body, and the fore body. Based on the obtained results, the water rise up at the mid-section of Model C2 is larger than that of Model C. In the fore body ($X = 0.6$), the water rise up of Model C is larger in the mid body. In the aft body, water rise up of Model C is also larger. This proves the fact that the step may lead to a decrease in the water rise up around the transverse sections locating at the aft of the steps.

The free surface elevation and wave patterns behind both Models are portrayed from top view at different Froude numbers in Fig. 13. As evident in this figure, the free surface elevation just behind the transom is larger for Model C in comparison with Model C2. At Froude number Fr = 2.395, the maximum free surface elevation of Model C2 is found to be 0.0075, while it is equal to 0.062 for Model C. At
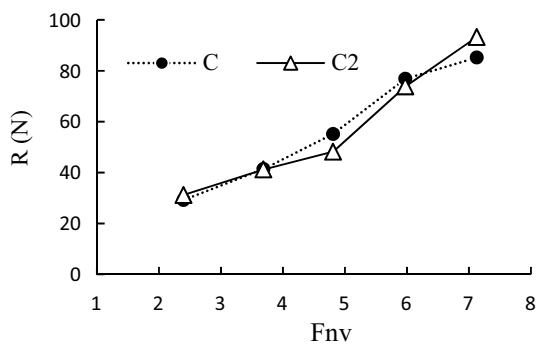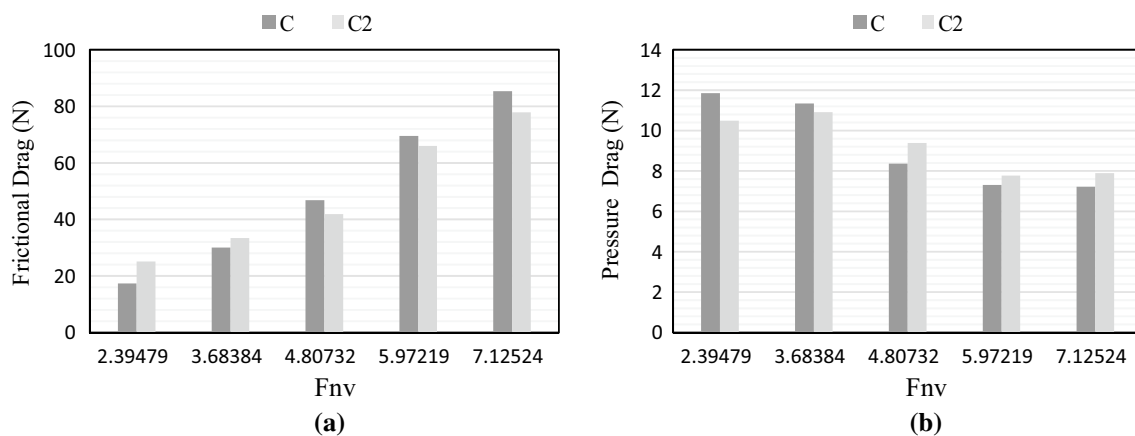
Fig. 9 Comparison of **a** frictional and **b** pressure resistance of Model C against Model C2
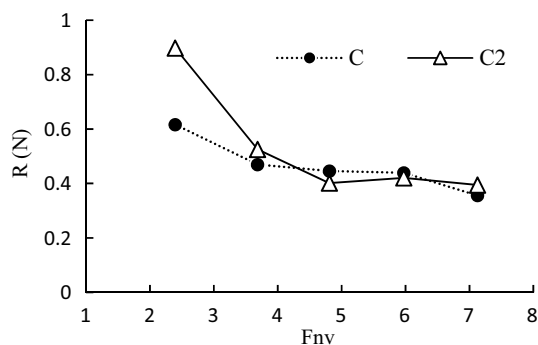

**Fig. 10** Comparison of the wetted surface of Model C against Model C2

Froude number Fr = 3.684, similar behavior is observed, again. Maximum water height behind Model C2 is found to be 0.075, while this height is 0.041 for Model C. Such differences are also evident at the other two larger Froude numbers. This is due to the fact that the shape of free surface behind the transom of a planing vessel is a function of trim angle of that surface, as reported by Savitsky and Morabito [5, 34]. For a stepped planing vessel, the body located behind the step has a local trim angle instead of the trim angle of the fore body, since it is exposed to a separated flow from the step right next to it. As a result, when the flow separates from the transom of the aft body, it leaves the transom with a higher trim angle which of course leads to a maximum water height.

4.3.4 Pressure distribution

The computed longitudinal pressure distribution over the center line of Models C and C2 is displayed in Fig. 14. The plots in this figure offer more information regarding the effect of a step on the pressure acting on the bottom of a planing hull. It is observed that three maximum pressures exist for the double-stepped model, while the non-step hull (Model C) exhibits only one maximum pressure. Existence of the step and separation of flow from it are the cause of this phenomenon. When the flow leaves a step, it attacks the next body with an angle of attack which itself leads to a new maximum pressure. It is also noteworthy that the first maximum pressure of Model C2 is larger than that of Model C. This happens due to the fact that Model C2 has larger equilibrium trim angle. It should be noted that Morabito [34] has previously described the pressure distribution acting on the bottom of planing hulls and has found that by increasing the trim angle, the maximum pressure is intensified. Plots in Fig. 14 also indicate that pressure distribution of Model C eventually increases after its first abrupt reduction and then becomes zero and vanishes at the transom. This is while such behavior is not evident for Model C2. These facts are supported by Savitsky [5] equation and the conclusions by Morabito [34]. Since Model C does not face any flow separation, hydrostatic pressure is involved in the wetted area near the transom. However, there are two flow separations at the bottom of Model C2, and hence hydrostatic pressure cannot be an effective contributor, and even leads to production of the lift force. A final point which should be made is the fact that pressure coefficient (Cp) decreases, as the Froude number increases. This can be attributed to the reduction in trim angle. As the speed increases, the trim angle of a planing hull (both stepped and non-stepped hulls) decreases. The previous formulations of Morabito [34] have verified that reduction of trim angle results in the reduction of pressure coefficient. In addition, pressure distribution over the entire wetted area of the planing hulls is shown in Fig. 15. As evident in this figure, similar to what is observed in Fig. 14, three maximum pressure areas exist on the bottom of the two-stepped planing hull (model C2), while

Fig. 11 Comparison of the shape of the wetted surface of Model C against Model C2 at Froude numbers: **a** Fr = 2.395, **b** Fr = 3.684, **c** Fr = 4.807, **d** Fr = 5.972 and **e** 7.125
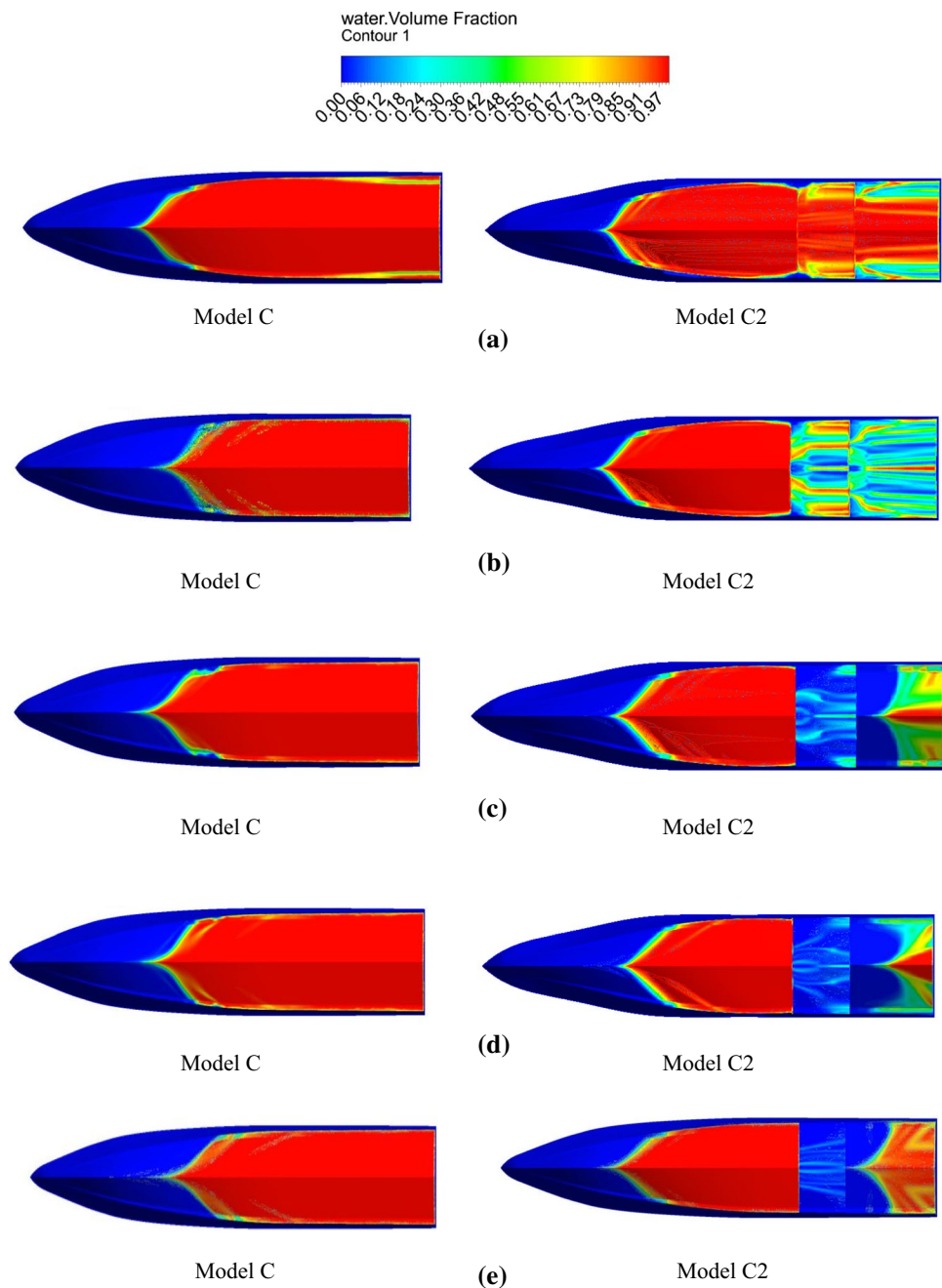
there is only one maximum pressure area on the bottom of model C (the non-stepped planing hull). This figure can also provide better understanding regarding the pressure values near the chine of two-stepped planing hulls and its differences with the non-stepped planing hulls. What is significant between non-stepped and double-stepped planing hull is that pressure values becomes also large in the proximity of chines in the double-stepped planing hulls. This may attributed to the separation of the water from the edge of the steps. When this phenomenon occurs, the flow becomes thicker from the top view, and thus produces larger pressure near the chines. However, it should be noted that the chine pressure becomes zero which matches with previous observations of Morabito [34].

5 Conclusions

In the current paper, flow around two planing hulls including a non-stepped model (Model C) and a double-stepped model (Model C2) is numerically simulated and their hydrodynamic characteristics are examined. The main aim of this study is to compare hydrodynamic characteristics and flow behavior of these planing hulls with each other, and then

Fig. 12 Water rise up around the transverse sections at Froude numbers: **a** Fr = 2.395, **b** Fr = 3.684, **c** Fr = 4.807, **d** Fr = 5.972 and **e** 7.125
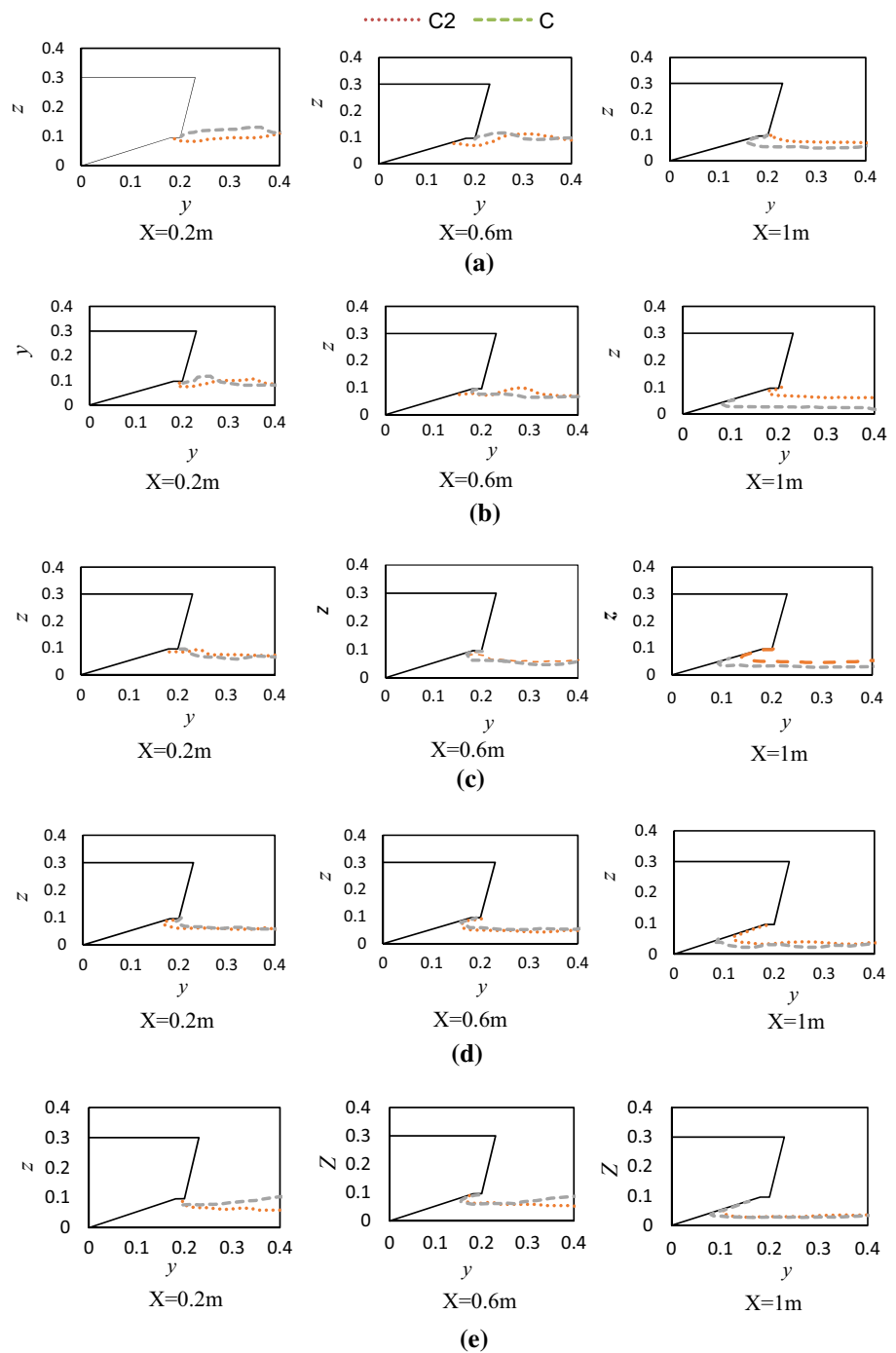
draw scientific conclusions regarding the influence of the steps at the bottom of these planing hulls in calm water. To conduct the targeted simulations, ANSYS-CFX is used which utilizes FVM based on FEM approach as well as SIMPLE scheme. Before embarking on the targeted simulations, a mesh study is carried out and an optimum mesh size is adopted.

The simulations are validated by comparing the numerically computed resistance against experimentally measured data associated with these hulls and good accuracy is displayed. Subsequently, the intended simulations are performed at five different Froude numbers and followings are concluded:

1. The resistance of both Models C and C2 are computed and it is shown that their resistances are approximately the same at the first two Froude numbers (i.e., Fr = 2.395 and Fr = 3.684). However, at the other larger Froude numbers (i.e., Fr = 4.807, Fr = 5.972 and Fr = 7.125), the
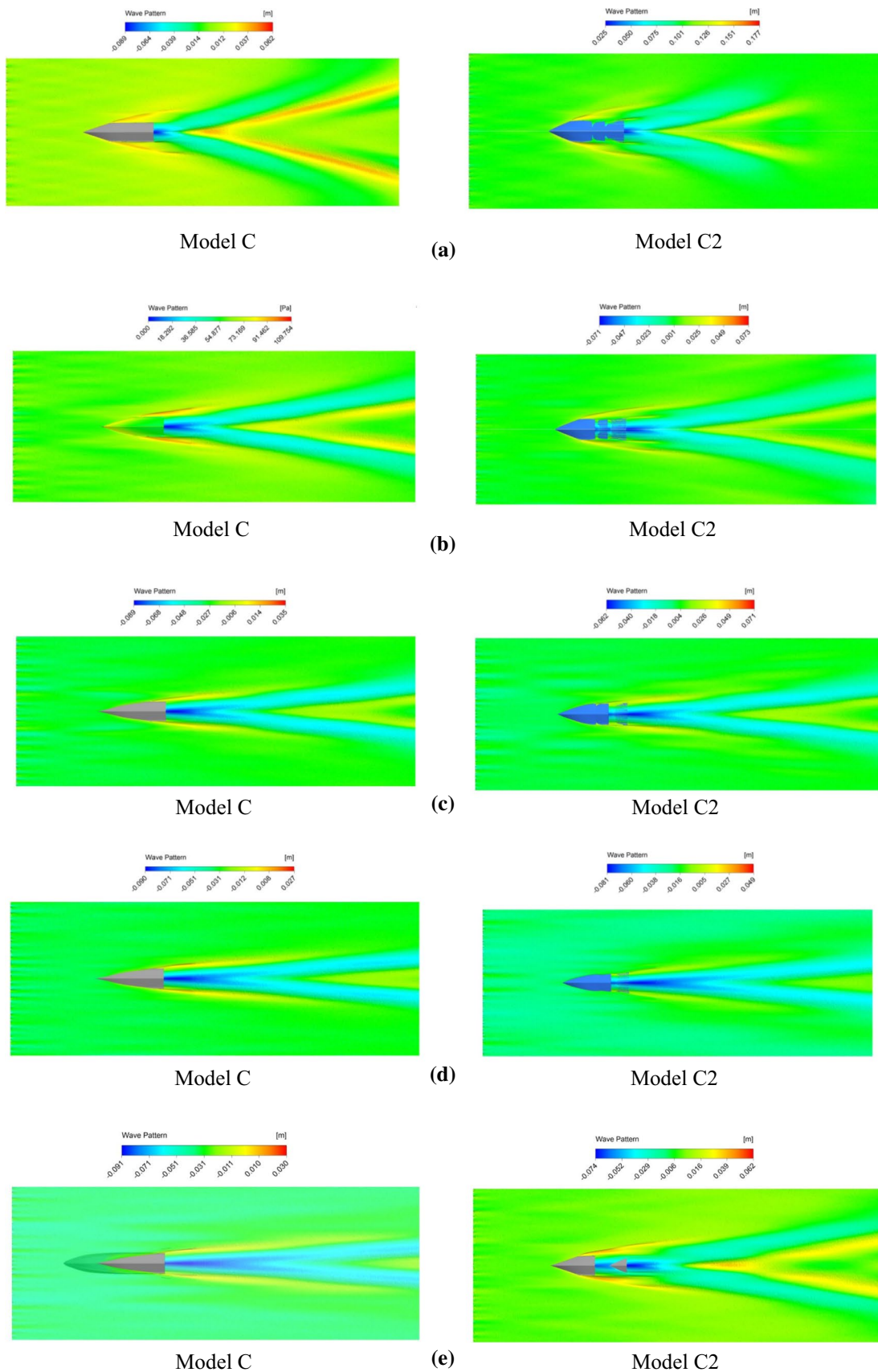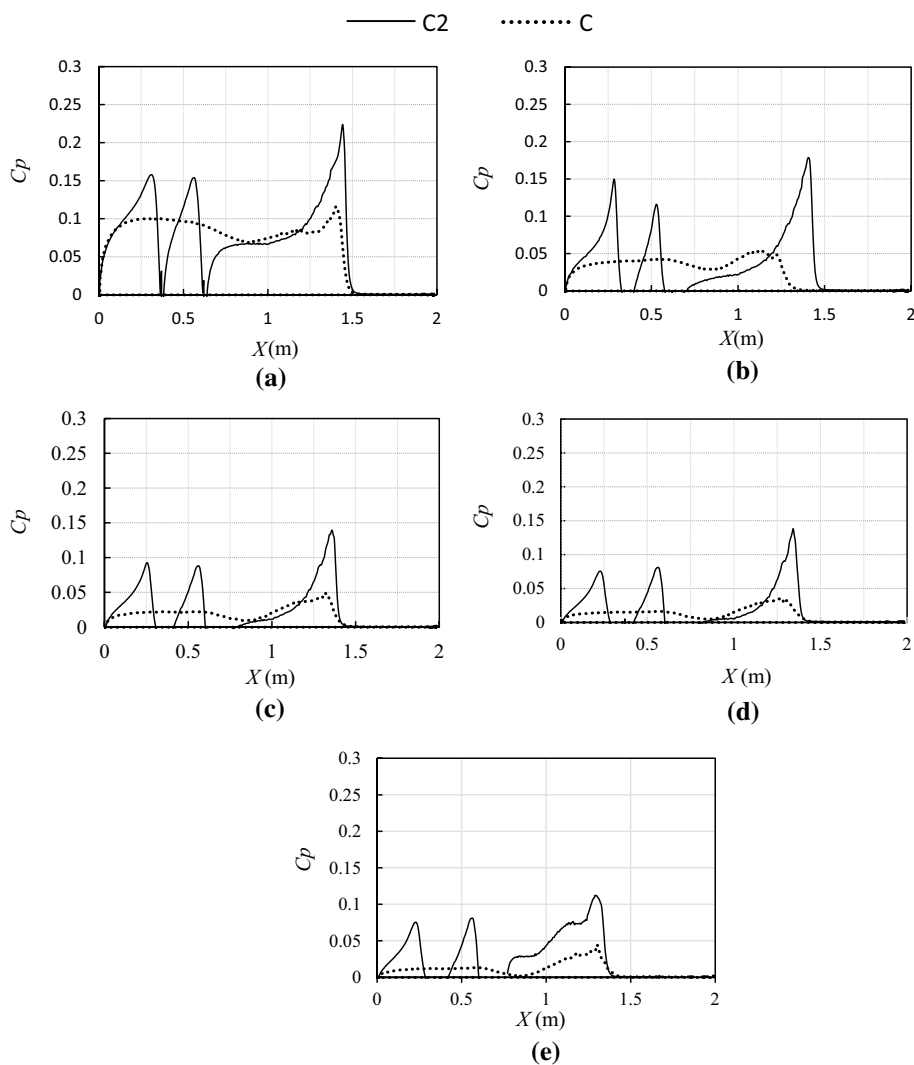
Fig. 13 Free surface from under hull body behind Models C and C2 at Froude numbers: **a** Fr = 2.395, **b** Fr = 3.684, **c** Fr = 4.807, **d** Fr = 5.972 and **e** 7.125

Fig. 14 Pressure distribution over the center line of Models C and C2 at: **a** Fr=2.395, **b** Fr=3.684, **c** Fr=4.807, **d** Fr=5.972 and **e** 7.125

1. resistance of Model C2 is smaller in comparison with that of Model C.

2. Pressure and frictional resistance components of the considered Models C and C2 are also computed and compared. The obtained results indicate that when the steps are added to the hull, the pressure drag increases, while the frictional component decreases.

3. The wetted surface profiles of the considered hull are also calculated and compared. Based on the obtained results, it is concluded that at Froude numbers Fr=2.395 and Fr=3.684), the step does not play any positive role and it even leads to larger wetted surface. However, as the Froude number increases (at Fr=4.807, Fr=5.972 and Fr=7.125), the wetted surface of the stepped planing hull becomes smaller.

4. Free surface elevations around the three transverse sections of both models are determined. The displayed results imply that the free surface around transverse sections of the fore body of Model C2 is raised up more in comparison with a transverse section of Model C located at the same longitudinal position. This is while the free surface is situated at a lower height in transverse sections of mid and aft body of C2 in comparison with those of Model C.

5. Water surface elevations behind the transom stern have also been displayed. It has been observed that the free surface behind the Model C2 elevates more in comparison with Model C2.

6. Pressure distribution over the center line of both models are computed and compared. The results are indicative of the fact that three pressure maximums occur. In addition, it is seen that first maximum pressure of Model C2 is larger than that of Model C. It is also observed that in the near-transom area of the non-stepped hull, the hydrostatic pressure becomes sensitive and contributes to the production of lift force, but for the stepped model, the hydrostatic pressure does not play any role.
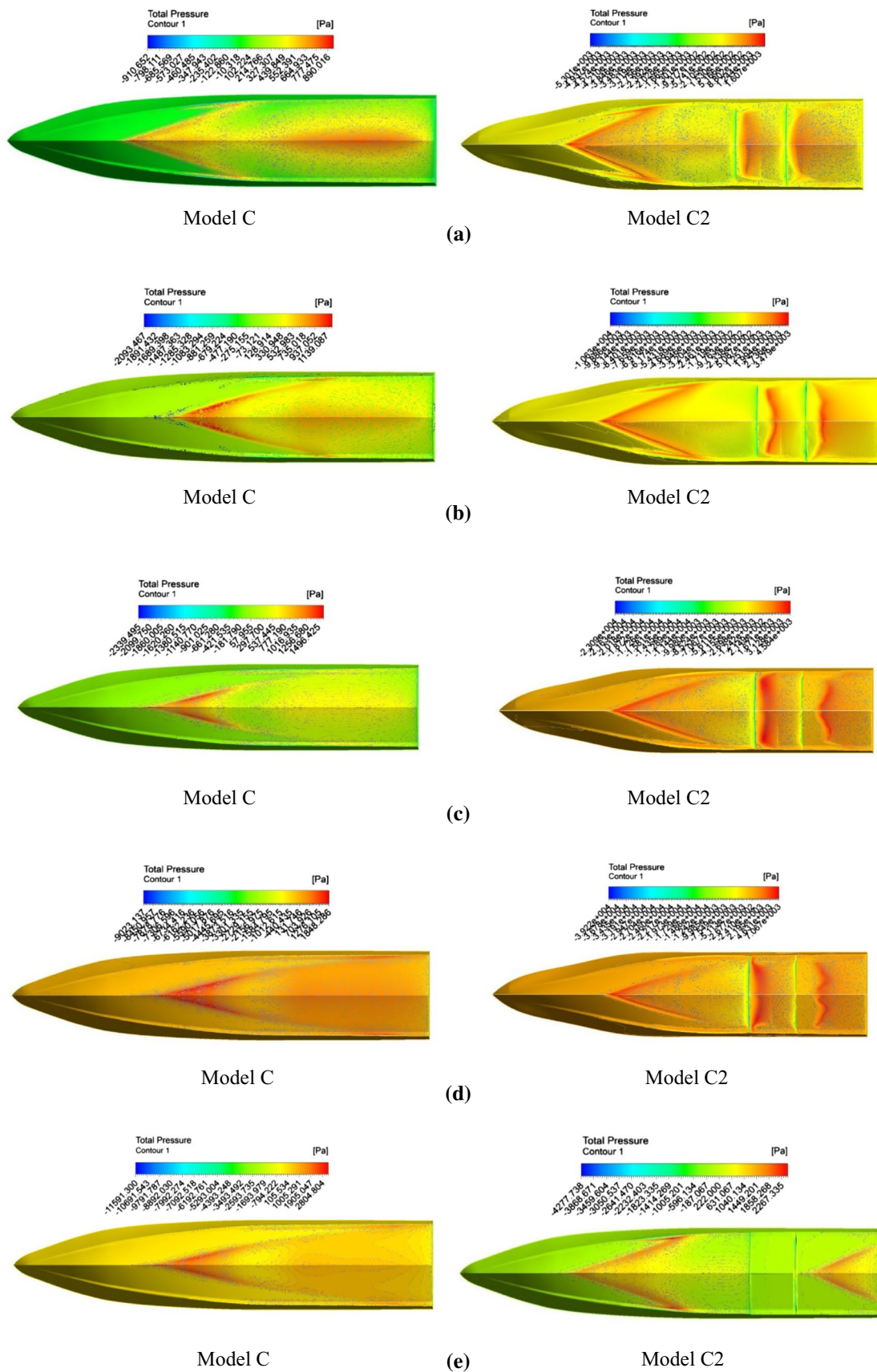
Fig. 15 Pressure distribution on the planing surface of Models C and C2 at Froude numbers: **a** Fr = 2.395, **b** Fr = 3.684, **c** Fr = 4.807, **d** Fr = 5.972 and **e** 7.125

Stepped planing hulls are found to have smaller drag, since flow separates from the steps and lead to reduction of the wetted surface which itself leads to significant reduction of frictional resistance. Meanwhile, they indicate some negative effects in their hydrodynamic performance in calm water like larger free water elevation behind the transom and larger hydrodynamic pressure that exists in their bow section. It should be mentioned that stepped planing hulls have a small variability of trim angle and improve the control of the longitudinal running attitude. From the economical point of view, the stepped planing hulls can be considered more efficient in their calm water operations than a non-stepped hull. However, there are some remaining concerns regarding these types of vessels. The first concern is related to their stability in transverse and horizontal planes which are reported to be the most important concerns of the previous researchers and engineers. The second concern is related to their motions in waves. As seen in the current paper, when larger pressure is produced in their bow section, larger vertical acceleration and impact pressure may occur. Therefore, future studies can involve the stability of the stepped planing hulls in transverse as well as horizontal planes and their vertical motions in head sea.

References

1. Kapryan WJ, Boyd GM (1955) Hydrodynamic pressure distribution obtained during a planing investigation of five related prismatic surfaces. NACA Technical Note 3477
2. Smiley RF (1950) A study of water pressure during landing with special reference to a prismatic model having a heavy loading and a 30-degree angle of deadrise. NACA Technical Note 2111
3. Green AE (1935) The gliding of a flat plate on a stream of finite depth part I. In: Proceedings of the Cambridge philosophical society
4. Green AE (1936) The gliding of a flat plate on a stream of finite depth part II. In: Proceedings of the Cambridge philosophical society
5. Savitsky D (1964) Hydrodynamic analysis of planing hulls. Mar Technol 1:71–95
6. Katayama T, Hayashita SH, Suzuki K, Ikead Y (2002) Development of resistance test for high-speed planing craft using very small model scale effects on drag force. J Kansai Soc Nav Archit 238:39–47
7. Blount DL, Fox DL (1976) Small-craft power prediction. Mar Technol 13:14–45
8. Svahn D (2009) Performance prediction of hulls with transverse steps. Dissertation, University of KTH
9. Grigoropoulos GJ, Loukakis TA (1995) Effect of spray rails on the resistance of planing hulls. In: 3rd international conference on fast sea transportation, Germany 1995
10. Pemberton R, et al (2001) A comparison of computational methods for planing crafts hydrodynamics. In: Proceedings of second international euro conference on high performance marine vehicles, HIPER 01'
11. Caponetto M (2001) Practical CFD simulations for planing hulls. In: Proceedings of second international euro conference on high performance marine vehicles, HIPER 01'
12. Brizzolara S, Serra F (2011) Accuracy of CFD codes in the prediction of planing surface hydrodynamic characteristics. In: INSEAN
13. DeLuca F, Mancini S, Miranda S, Pensa C (2016) An extended verification and validation study of CFD simulations for planing hulls. J Sh Res 60:101–118
14. Azcueta R (2004) Steady and unsteady RANSE simulations for littoral combat ships. In: Proceedings of 25th symposium on naval hydrodynamics
15. Jiang Y, Sun H, Zou J, Hu A, Yang J (2016) Analysis of tunnel hydrodynamic characteristics for planing trimaran by model tests and numerical simulations. Ocean Eng 113:101–110
16. Ghadimi P, Loni A, Nowruzi H, Dashtimanesh A, Tavakoli S (2014) Parametric study of the effects of trim tabs on running trim and resistance of planing hulls. Adv Sh Ocean Eng 3:1–12
17. Ghadimi P, Dashtimanesh A, Feizi Chekab M (2016) Introducing a new flap form to reduce the transom waves using a 3-D numerical analysis. Int J Comput Sci Eng 12:265–275. https://doi.org/10.1504/IJCSE.2016.076934
18. Ghadimi P, Dashtimanesh A, Faghfoor Maghrebi Y (2013) Initiating a mathematical model for prediction of 6-DOF motion of planing crafts in regular waves. Int J Eng Math 2013:853793. https://doi.org/10.1155/2013/853793
19. Seif MS, Mousavirad SM, Sadat Hosseini SH (2004) The effect of asymmetric water entry on the hydrodynamic impact. Int J Eng 17:205–212
20. Yousefi R, Shafaghat R, Shakeri M (2013) Hydrodynamic analysis techniques for high speed planing hulls. J Appl Ocean Res 42:105–113
21. Taunton DJ, Hudson DA, Shenoi RA (2011) Characteristics of a series of high-speed hard chine planing hulls-part I: performance in calm water. Int J Small Cr Technol 152:55–75
22. Lee E, Pavkov M, McCue-Weil L (2014) The systematic variation of step configuration and displacement for a double-step planing craft. J Sh Prod Des 30:89–97
23. Timmins CR (2014) Yaw stability of a recreational stepped planing hull. Trans Soc Nav Archit Mar, Eng
24. Morabito MG, Pavkov ME (2014) Experiments with stepped planing hulls for special operations craft. Trans Roy Inst Naval Archit Part B Int J Small Cr Technol 156:87–97. https://doi.org/10.3940/rina.ijsct.2014.b2.162
25. Matveev K, Bari G (2015) Effect of deadrise angles on hydrodynamic performance of a stepped hulls. In: Proceedings of the Institution of Mechanical Engineers Part M Journal of Engineering for the Maritime Environment
26. Matveev K (2012) Transom effect on the properties of an air cavity under a flat-bottom hull. J Sh Offshore Struct 7:143–149
27. Matveev K (2015) Hydrodynamic modeling of semi-planing hulls with air cavities. Int J Nav Archit Ocean Eng 7:500–508
28. Garland W, Maki KJ (2012) A numerical study of a two-dimensional stepped planing surface. J Sh Prod Des 28:60–72. https://doi.org/10.5957/JSPD.28.2.120005
29. Makasyeye M (2009) Numerical modeling of cavity flow on bottom of a stepped planing hull. In: Proceeding of the 7th international symposium on cavitation, Ann Arbor, USA 2009
30. Lotfi P, Ashrafizaadeh M, Kowsari Esfahan R (2015) Numerical investigation of a stepped planing hull in calm water. J Ocean Eng 94:103–110
31. Ghadimi P, Tavakoli S, Dashtimanesh A, Zamanian R (2016) Steady performance prediction of a heeled planing boat in calm water using asymmetric 2D+t model. In: Proceedings of the Institution of Mechanical Engineers, Part M: Journal of Engineering for the Maritime Environment
32. Akers RH (1999) Dynamic analysis of planing hulls in vertical plane. In: Proceedings of Naval Architects and Marine Engieering

33. Van Deyzen A (2008) A nonlinear mathematical model for motions of a planing monohull in head seas. In: Proceedings of the 6th international conference on high performance marine vehicles, Italy 2008

34. Morabito MG (2014) Empirical equations for planing hull bottom pressure. J Sh Res 58:185–200

35. Versteeg HK, Malalasekera W (2007) An introduction to computational fluid dynamics: the finite volume method. Pearson Education, Glasgow

36. Veysi SJ, Bakhtiari M, Ghassemi H, Ghiasi M (2015) Toward numerical modeling of the stepped and non-stepped planing hull. J Braz Soc Mech Sci Eng 37:1635–1645

37. DeMarco A, Mancini S, Miranda S, Scognamiglio R, Vitiello L (2017) Experimental and numerical hydrodynamic analysis of a stepped planing hull. J App Ocean Res 64:135–154